

INTEGRATION OF PHOTOSYSTEM I WITH CARBON-BASED MATERIALS FOR
SOLAR ENERGY CONVERSION DEVICES

By

Kevin M. Winter

Thesis

Submitted to the Faculty of the

Graduate School of Vanderbilt University

in partial fulfillment of the requirements

for the degree of

MASTER OF SCIENCE

in

Chemistry

August, 2014

Nashville, Tennessee

Approved:

David Cliffler, Ph.D.

Kane Jennings, Ph.D.

ACKNOWLEDGEMENTS

This work would not have been possible without the financial support of Vanderbilt University, the Vanderbilt Institute for Chemical Biology Fellowship Award, and the Scialog Program from the Research Corporation for Science Advancement. I am especially thankful for the guidance and everyday support of Dr. David Cliffler and Dr. Gabriel Leblanc.

I am grateful to everyone I worked with in the Cliffler group for all the ways you have helped me, large and small, over the last two years. I, very honestly, would not have been able to complete this work without you all, because I could never find anything in the lab on my own.

Lastly, I would like to thank, in particular, my dear friends that I have made at Vanderbilt. Amy Poynter and Chatney Spencer, thank you so much for pushing and encouraging me. I hope I've done the same for you.

TABLE OF CONTENTS

	Page
Acknowledgements.....	ii
List of Tables	v
List of Figures	vi
Chapter 1: Introduction to Photosystem I.....	1
1.1 The Global Energy Crisis.....	1
1.2 Photosynthesis and Photosystem I	2
1.3 Incorporation of Photosystem I into Photovoltaic Devices.....	3
1.4 Toward Efficient, Low Cost, Carbon-Based Electrode Materials	5
Chapter 2: General Experimental and Analytical Methods	6
2.1 Photosystem I Extraction and Isolation.....	6
2.2 Optical Characterization of Photosystem I.....	8
2.3 Deposition of Photosystem I Multilayer Films	9
2.4 Electrochemical Analysis of Biohybrid Electrodes.....	11
Chapter 3: Graphene Oxide and Reduced Graphene Oxide as a Supporting Matrix for Photosystem I.....	13
3.1 Graphene, Graphene Oxide, and Reduced Graphene Oxide.....	13
3.2 Interfacing Photosystem I with Graphene Oxide and Reduced Graphene Oxide	14
3.3 Results and Discussion.....	15
3.4 Conclusions	17
3.5 Experimental	17
3.5.1 Photosystem 1 Extraction and Isolation.....	17
3.5.2 Preparation of PSI-RGO Composites	17
3.5.3 Hydrofluoric Acid Etching of Silicon Substrates	18
3.5.4 Deposition of Composite Films onto Etched Silicon Substrates	19
3.5.5 Raman Analysis of Composite Films	19
3.5.6 Profilometry	20
3.5.7 Electrochemical Analysis of Composite Biohybrid Electrodes.....	21
Chapter 4: Reduced Graphene Oxide as a Transparent Electrode with Photosystem I Films	22
4.1 Transparent Electrodes and Opaque Mediators.....	22

4.2 Reduced Graphene Oxide as a Transparent, Conductive Electrode.....	22
4.3 Results and Discussion.....	23
4.4 Conclusions	26
4.5 Experimental	27
4.5.1 Photosystem 1 Extraction and Isolation.....	27
4.5.2 Preparation of RGO Electrodes	27
4.5.3 Deposition of PSI Multilayer Films on RGO Electrodes.....	28
4.5.4 Electrochemical Analysis of PSI-modified RGO Electrodes	28
4.5.5 Profilometry	29
4.5.6 Transmitted Light Intensity Measurements	29
References.....	31
Curriculum Vitae	35

LIST OF TABLES

	Page
Table 1. Power of transmitted light passed through subsequent layers of the electrochemical cell	29

LIST OF FIGURES

	Page
Figure 1. A model of plant PSI in the thylakoid membrane	3
Figure 2. Energy diagram of electron flow from p-Si to the Pt counter electrode	5
Figure 3. Photocurrents reported by the Cliffel and Jennings research groups over time	5
Figure 4. General procedure for the extraction of PSI protein complex from plant material.....	7
Figure 5. UV-Vis spectrum of PSI in solution.....	9
Figure 6. Diagram of the dropcast deposition of aqueous PSI protein complex onto a substrate .	10
Figure 7. Electrochemical cell setup and illumination source	11
Figure 8. Sample photochronoamperometric analysis of PSI-modified electrode	12
Figure 9. Two-dimensional molecular structure of graphene, GO, and RGO	13
Figure 10. Photochronoamperometry curves of PSI and PSI-RGO composite films on etched p-Si substrates.....	15
Figure 11. Cyclic voltammogram of PSI and PSI-RGO composite films on etched p-Si substrates	16
Figure 12. UV-Vis spectra of the reduction of GO to RGO at 0 h and 24 h	18
Figure 13. Raman spectra showing reduction of GO to RGO and confocal microscope images of PSI-GO and PSI-RGO composite films on p-Si substrates	20
Figure 14. Diagram of the PSI-modified RGO electrode	23
Figure 15. Photochronoamperometric measurements of RGO and PSI-modified RGO electrodes	24
Figure 16. Photochronoamperometric measurements of different mediator solutions.....	25
Figure 17. Film thickness of RGO electrodes as a function of the number of deposition steps....	26
Figure 18. Average power measurements of light transmitted through layers of the electrochemical cell	26
Figure 19. Diagram of the production of conductive RGO electrodes on glass substrates	28

CHAPTER 1

Introduction to Photosystem I

1.1 The Global Energy Crisis

In 2006, approximately 86% of the globe's 500 exajoule energy consumption was satisfied by fossil fuels, and this energy requirement is expected to increase 44% to 720 exajoules by the year 2030.¹ Unfortunately, reliance on these fuels as the major energy source for our civilization is growing increasingly unsustainable. Several problems have developed out of our dependence on fossil fuels, the most obvious of which include an insufficient supply of the fuel and climate changes.¹ Therefore, there is an urgent need for the development of alternative, sustainable sources of energy. One promising area of research in this field is solar energy. In 2001, less than 0.1% of electricity produced was derived from a solar source, despite the fact that more energy strikes the earth's surface from the sun in one hour than is used globally in one year.^{2,3} Of the 1.7×10^5 TW of energy delivered to the earth by the sun, it is estimated that about 600 TW of global solar energy could be practically harvested. Developing and utilizing solar energy conversion devices of as little as 10% efficiency, then, could produce nearly 60 TW of power, much more than the current global need.⁴ Unfortunately, due to the current affordability of fossil fuels, even a device that functioned at the Shockley-Queisser Limit of ~30% efficiency (the theoretical limit) would face difficulty finding widespread adoption if it was not cost effective.³ Therefore, not only is there a need for efficient solar energy conversion devices to displace current fossil fuel use, the needed devices must also be affordable. To find machinery that meets both of these specifications we need look no further than nature itself.

1.2 Photosynthesis and Photosystem I

Photosynthesis is the biological process by which algae, higher plants, and cyanobacteria convert solar radiation into a stored chemical energy source in the form of carbohydrates. This energy is then consumed by animals or stored as fossil fuels, positioning the sun as the energy source for nearly all life on the planet.⁵ The process of photosynthesis progresses through a series of steps including light absorption, water splitting, charge separations, and an electron transport mechanism that leads to the formation of these high energy carbon reserves. Nature has been perfecting its photosynthetic pathway for thousands of years and has developed a set of photoelectrochemical protein complexes to accomplish it. Photosystem I (PSI), one of these complexes, is a thylakoid membrane protein complex composed of 16 protein subunits, 167 light harvesting chlorophyll, a reaction center and an internal electron transfer chain.⁶ The antennae chlorophyll absorb light of specific energies which are then used to excite an electron in the P700 reaction center. This excited electron is then rapidly shuttled ($1\mu\text{s}$) through the electron transport chain to the F_B iron-sulfur complex (Figure 1).^{6,7} PSI creates and stabilizes these charge separations with a quantum efficiency near unity.⁸

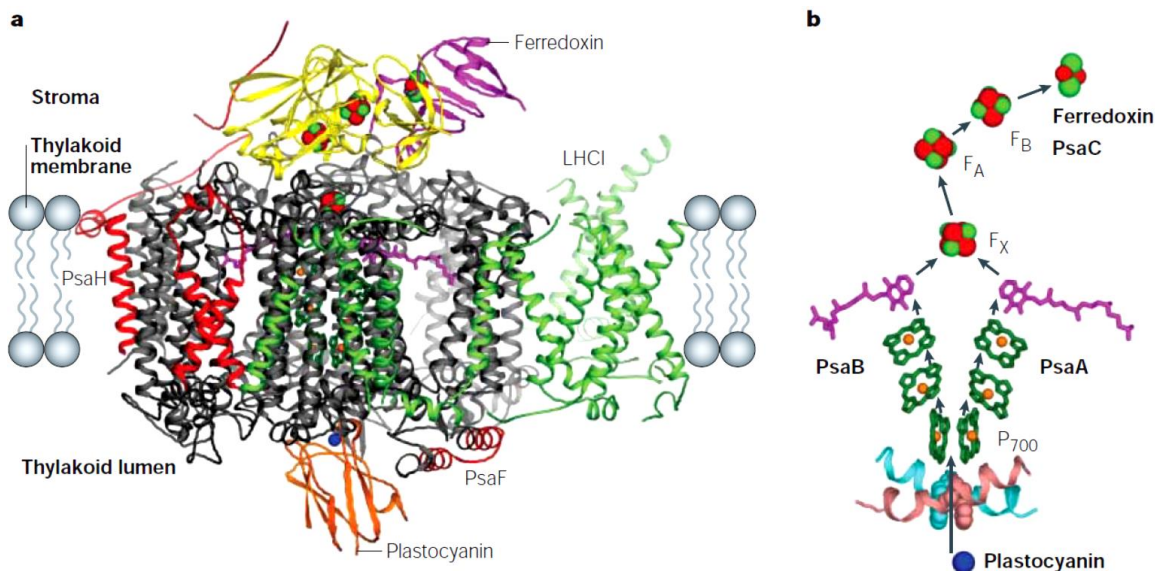


Figure 1. A model of plant PSI in the thylakoid membrane (a) and the cofactors involved in the charge separation mechanism (b). Image reproduced from Reference 9 with permission from Nature Publishing Group.

1.3 Incorporation of Photosystem I into Photovoltaic Devices

PSI has gained attention globally as a potential photoactive material in devices due to its efficiency and ease of availability. The first reported work to this end was in 1985 by Greenbaum and co-workers, who precipitated colloidal platinum onto the thylakoid membranes of chloroplasts and observed sustainable hydrogen and oxygen gas evolution under illumination.¹⁰ This work was later expanded upon by several groups using isolated PSI protein complexes.^{11–13} A study in 1997 by Lee *et al.* reported that individual PSI complexes could function as photodiodes,¹⁴ which sparked further studies of the electrochemical properties of PSI.¹⁵ A solid-state device incorporating the protein was developed in 2004.¹⁶

The Cliffel and Jennings groups at Vanderbilt University have been studying the electrochemical properties of PSI and its use in functional photovoltaic devices for over a decade. The work began with the first characterization of PSI adsorbed onto gold electrodes

using patterned self-assembled monolayers (SAMs).^{17,18} These photocurrents were increased by the development of a method of forming dense monolayers of PSI quickly and directly onto gold electrodes using vacuum deposition.¹⁹ Photocurrents produced by these films were limited, however, by the mixed orientation of the proteins which negated much of the observed current. Nanoporous gold leaf was used as an increased surface area electrode to further enhance PSI-mediated electron transfer.²⁰ Thick, multilayer PSI films showed an additional, dramatic increase in generated photocurrent. These films form a protein matrix that is permeable to electrochemical mediators and has a high concentration of the photoactive reaction centers in an environment similar to the thylakoid stacks found in chloroplasts.^{21,22} The use of semiconductors, specifically p-doped silicon (p-Si), were found to produce an even greater photocurrent increase due to alignment of the p-Si valence band with the P700 site and the conduction band with the F_B site of PSI. The doping lowers the Fermi level of the Si which promotes electron flow from p-Si to the P700 reaction center where it is then excited by incident light and carried to the counter electrode by an electrochemical mediator (Figure 2).²³ Our group has reported increases in photocurrents of over five orders of magnitude since work began using PSI (Figure 3).²⁴

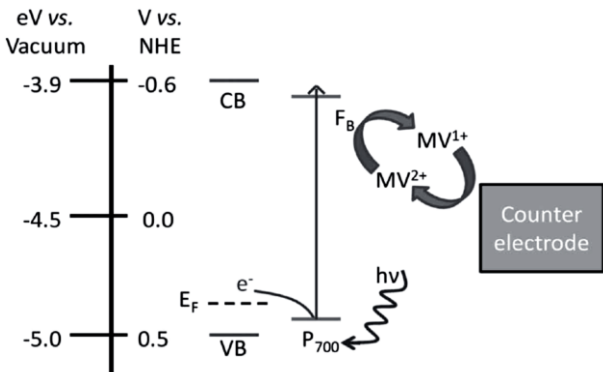


Figure 2. Energy diagram of electron flow from p-Si to the platinum counter electrode. Image adapted from Reference 23 with permission of John Wiley and Sons.

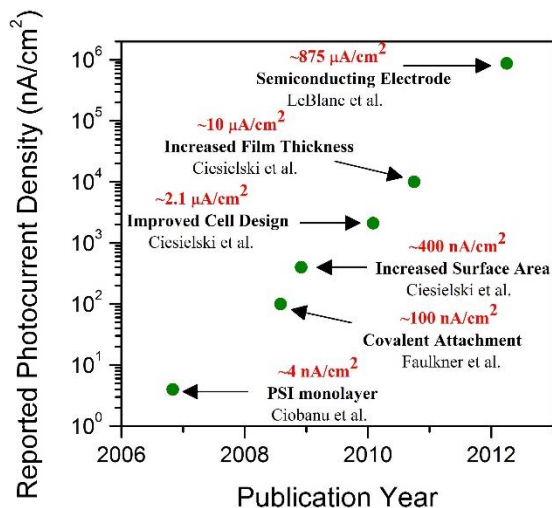


Figure 3. Photocurrents reported by the Cliffel and Jennings research groups over time. Image adapted from Reference 24 with permission from the American Chemical Society.

1.4 Toward Efficient, Low Cost, Carbon-Based Electrode Materials

The materials used to assemble the photocells previously studied in our group, specifically the electrode materials such as the noble metals, can unfortunately be quite expensive. In order for these alternative energy devices to find widespread adoption, they must be both efficient and cost effective. The objective of this thesis is to detail progress made toward the development of low cost, carbon-based electrodes utilizing graphene oxide (GO) and reduced graphene oxide (RGO) as a conductive matrix environment and a transparent, conductive electrode, respectively.

CHAPTER 2

General Experimental and Analytical Methods

2.1 Photosystem I Extraction and Isolation

Methods for the extraction of thylakoid membranes from higher plants were reported in 1980 by Reeves and Hall.²⁵ Subsequent isolation of PSI protein complexes was accomplished using a hydroxylapatite column as previously demonstrated by Shiozawa *et al.*²⁶ Using *Spinacea oleracea* (spinach) as a starting material, our group has adapted these protocols for the isolation of PSI for use in biohybrid electrodes, as previously reported.²⁷ Briefly, baby spinach was purchased at a grocery store and deveined, leaving only the leafy mass. The leaves were macerated in a grinding buffer using a blender and filtered twice through 2- and 8-layered cheesecloth, with the filtrate being chilled in order to limit PSI degradation due to proteolytic enzymes released upon maceration. The filtrate was then centrifuged at 8000 x g for 5 s and the supernatant poured off. The pellet was resuspended in buffer and a 1% surfactant solution and centrifuged a second time at 20000 x g for 15 min. The supernatant was then passed through a chilled hydroxylapatite column to purify the protein extract (Figure 4). The resulting PSI extract was then stored in aliquots at -80 °C. For the deposition of PSI multilayer films, an additional dialysis step using a 1:2000 mL PSI:water ratio must be performed to remove excess surfactant that helps to solubilize the film in aqueous solutions.²¹ Using these methods, our group has obtained PSI aliquots with concentrations ranging from 0.1-10 μM .²⁸

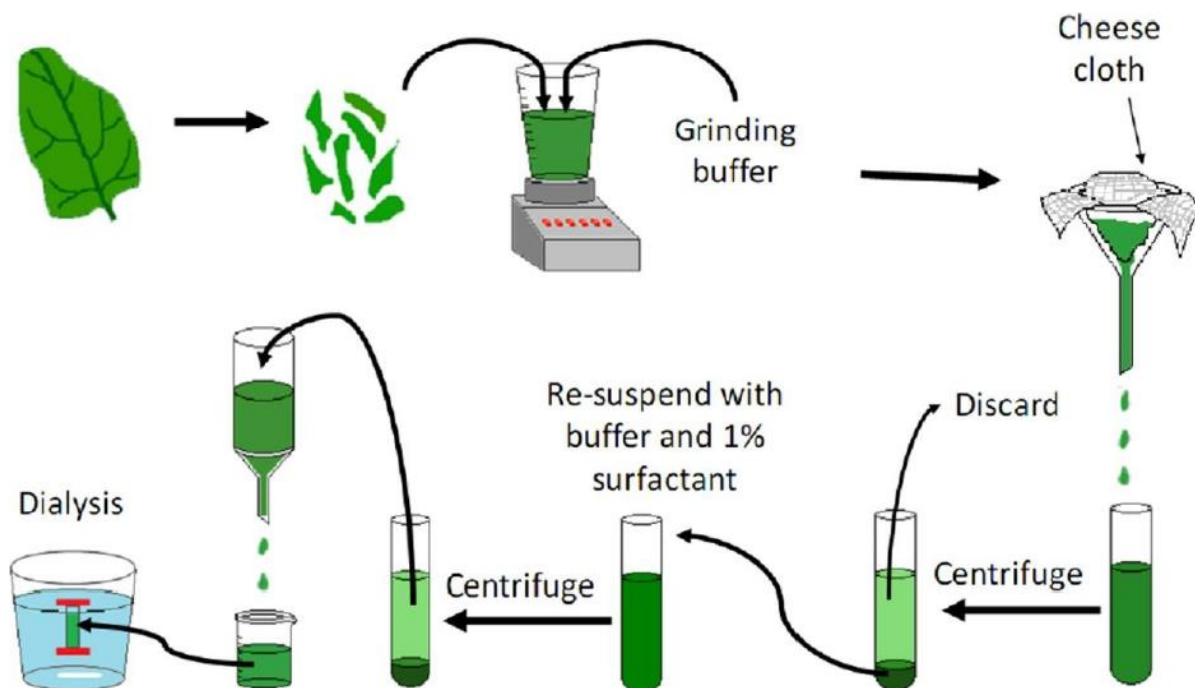


Figure 4. General procedure for the extraction of PSI protein complex from plant material, adapted from the work of Reeves and Hall,²⁵ Shiozawa *et al.*,²⁶ and Ciesielski *et al.*²¹ Image used from Reference 24 with permission from the American Chemical Society.

Due to the potential widespread adoption of PSI into photovoltaic devices, an area of concern has developed over the use of food sources such as spinach. It was hypothesized that PSI from any higher plant would function identically. Therefore, a study was done by Gunther and coworkers to attempt to extract PSI from *Pueraria lobata* (kudzu), an invasive vine that covers over 800,000 hectare of land in the southern United states and is rapidly spreading, causing widespread environmental damage by overtaking local crops and forests.²⁹ Following extraction methods identical to those used for spinach, Gunther was able to show that PSI protein could be harvested from kudzu starting materials, and that an enhancement in photocurrent could be seen on PSI-functionalized p-Si vs p-Si comparable to that seen using spinach sources. Although the protein concentrations were an order of magnitude lower than with spinach, this was an

interesting proof of concept study that confirmed the possible use of other, non-food source plant materials for PSI harvesting.

2.2 Optical Characterization of Photosystem I

Spectroscopy is the study of the interactions between matter and electromagnetic radiation. Incident photons are absorbed by the material of interest, causing it to move from its lower, initial energy state, E_i , to an excited state, E_f . The difference in energy between these states is exactly equal to the energy of the incident radiation and can be expressed using Equation 1, where h is Planck's constant, ν is the frequency of radiation, c is the speed of light, and λ is the wavelength of absorbed radiation.

$$\Delta E = E_f - E_i = h\nu = \frac{hc}{\lambda} \quad (\text{Equation 1})$$

Photosystem I interacts with light comprising a large range of the visible spectrum, absorbing strongly in the blue region (Soret) and red region (Q_y) (Figure 5). This wide window is particularly desirable for use in solar energy conversion devices. It is also useful for easy characterization measurements of PSI extracts and films. UV-Vis spectroscopy can be used to determine the P700 concentration based on the work of Baba *et al.*³⁰ as well as the chlorophyll a/b ratio using the method reported by Porra in 2002.³¹ Protein concentration or film thickness can also be determined based on absorbance intensities, as the material follows the Beer-Lambert law (Equation 2), which states that absorbance, A , is related to the extinction coefficient of the material, ε , the path length of the cell, l , and the concentration, c .²¹

$$A = \varepsilon * c * l \quad (\text{Equation 2})$$

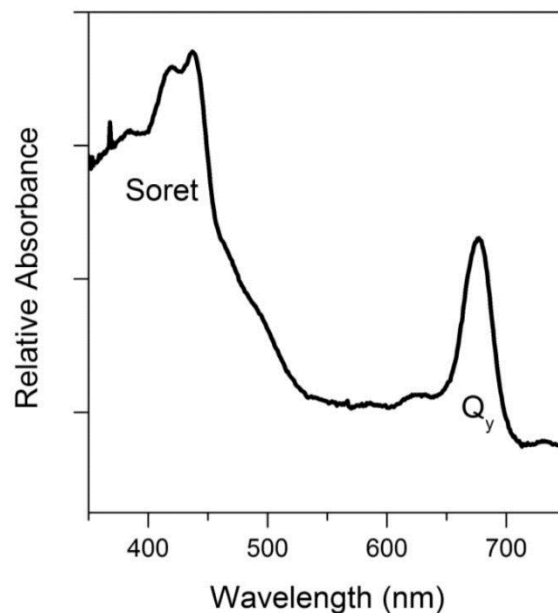


Figure 5. UV-Vis spectrum of PSI in solution with Soret and Q_y bands highlighted. Image used from Reference 28 with permission from Gabriel Leblanc.

2.3 Deposition of Photosystem I Multilayer Films

Substrates used for the electrode surface in biohybrid photovoltaic devices utilizing PSI are typically metals or metal oxides, often gold. Recent work in our group has shown that semiconductors, such as p-Si, greatly enhance photocurrent in conjunction with PSI.²³ Thick, multilayer films of the protein additionally showed a dramatic current enhancement due to their ability to capture more incident photons.²¹ For this reason, it is these types of films that were used for this work.

Photosystem I samples were extracted and dialyzed, as mentioned in Section 2.1. The substrate was cut to the desired size, and an opaque, adhesive mask was applied to it with a cutout area for the deposition of the protein. A 50 μ L aliquot of PSI was pipeted onto the substrate and the sample was placed under vacuum. The reduced pressure works to rapidly remove water from the PSI solution and concentrate the protein into a film. This process was

then repeated until the desired film thickness was achieved, with each deposition increasing the thickness by ~390 nm (Figure 6).²¹

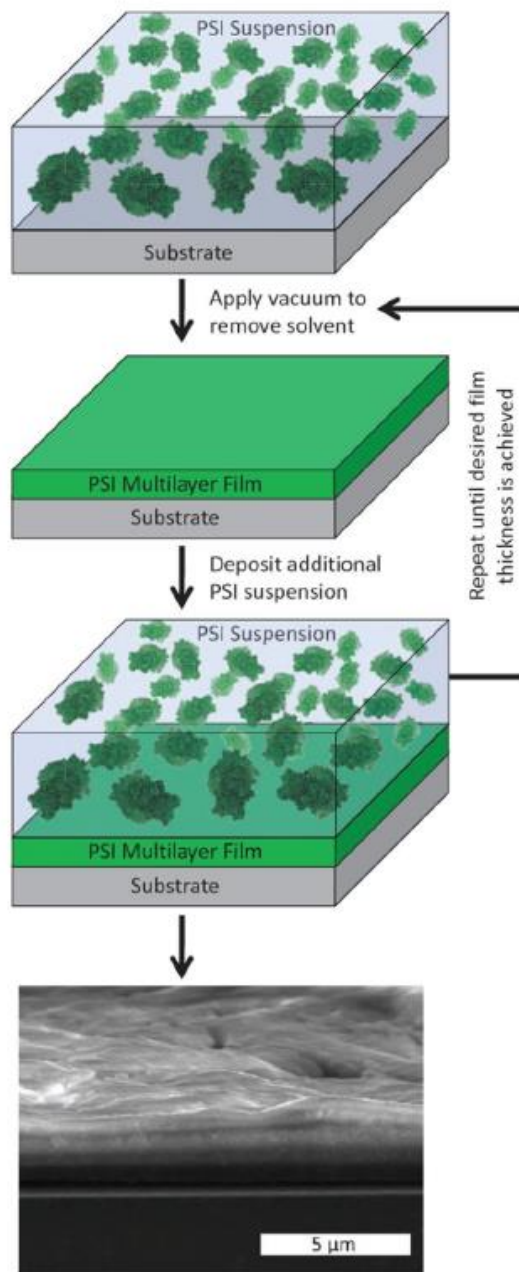


Figure 6. A diagram of the dropcast deposition of aqueous PSI protein complexes onto a substrate under vacuum to produce thick, multilayer protein films. The process can be repeated until the desired film thickness is achieved. Image used from Reference 21 with permission of John Wiley and Sons.

2.4 Electrochemical Analysis of Biohybrid Electrodes

A 3-electrode set-up (Figure 7) was used for the electrochemical analyses of these protein films. A platinum mesh was used as the counter electrode with a Ag/AgCl reference electrode. The biohybrid electrodes being studied acted as the working electrode. A redox mediator solution containing 100 mM KCl and a mediator species at low concentration was used to connect the electrodes. In a systematic study of mediator species, it was found that selection of a mediator with more positive formal potential showed better electron transfer to the counter electrode. This trend did not apply to methylene blue (MB) or 2,6-dichlorophenolindophenol (DCPIP), which have formal potentials of -0.2 V and 0.09 V (vs Ag/AgCl), because these mediators form dark blue solutions which absorb in the same range as PSI.³² Work to circumvent this problem will be detailed in Chapter 4. The electrochemical cell was assembled in a custom, transparent holder such that light could easily reach the sample. All electrochemical data was collected using a CH Instruments CHI 660a electrochemical workstation equipped with a

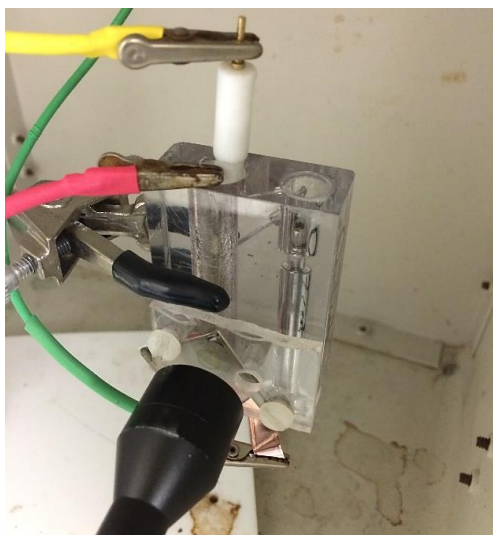


Figure 7. Electrochemical cell setup and illumination source. The PSI-modified working electrode is connected to the green clip, the Pt counter electrode to the red clip, and the Ag/AgCl reference electrode to the yellow clip.

Faraday cage. Illumination of the sample was achieved using a 250 W Leica KL 2500 LCD cold light source.

Photochronoamperometry is routinely performed to measure the photocurrent produced by PSI biohybrid electrodes.^{24,29,32} These experiments are performed by holding the working electrode at the open circuit potential (OCP), the potential at which there is no current flow under dark conditions. Though the OCP can vary drastically based on the surface modification of the electrode, conducting the experiments under these conditions ensures that no over-potential is applied to the samples, allowing the samples to be compared to one another. During the experiment, the sample is illuminated for a short time (~20 s) and the photocurrent is measured (Figure 8.). The photocurrent observed decays according to the Cottrell equation (Equation 3), where i is the current, n is the number of electrons transferred, F is Faraday's constant, A is the surface area of the electrode, D is the diffusion coefficient of the electrochemical mediator, C is

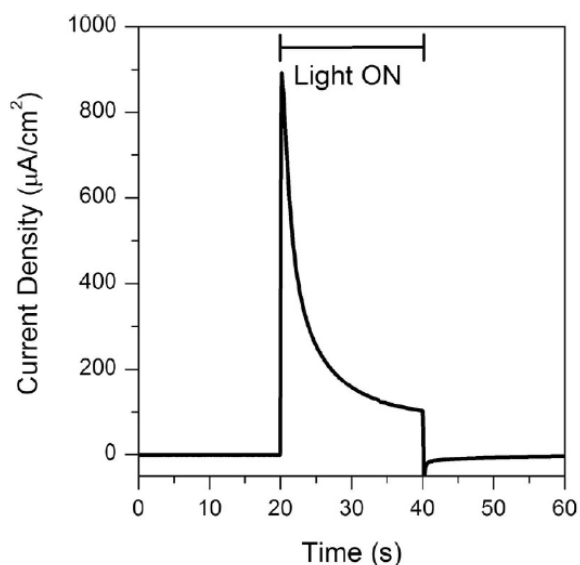


Figure 8. Sample photochronoamperometric analysis of a PSI-modified electrode. The sample was held at the OCP under dark conditions and then illuminated for 20 s. Image used from Reference 24 with permission from the American Chemical Society.

the concentration of the electrochemical mediator, and t is time. Current values were typically sampled after 10 s of illumination.

$$i(t) = \frac{nFAD^{1/2}C}{\pi^{1/2}t^{1/2}} \quad (\text{Equation 3})$$

CHAPTER 3

Graphene Oxide and Reduced Graphene Oxide as a Supporting Matrix for Photosystem I

3.1 Graphene, Graphene Oxide, and Reduced Graphene Oxide

Graphene is a single atom thick, two-dimensional sheet of sp^2 -hybridized carbon atoms (Figure 9) that has attracted a lot of interest upon its discovery due to its unique properties, such as high charge carrier mobility and zero effective mass, record high thermal and electrical conductivity, high elasticity, high transparency in the visible region of light, and impermeability to gases.³³⁻³⁵ While graphene as a material is very exciting, the process of obtaining pristine monolayer films of the substance can be difficult and time consuming. The first reported method was detailed by Novoselov *et al.* in 2004.³⁶ Mechanical exfoliation, or the “Scotch tape method” as it has become popularly referred to, can be used to obtain small areas of pristine monolayer graphene by repeatedly using tape to remove layers from highly ordered pyrolytic graphite until only a single monolayer remains.

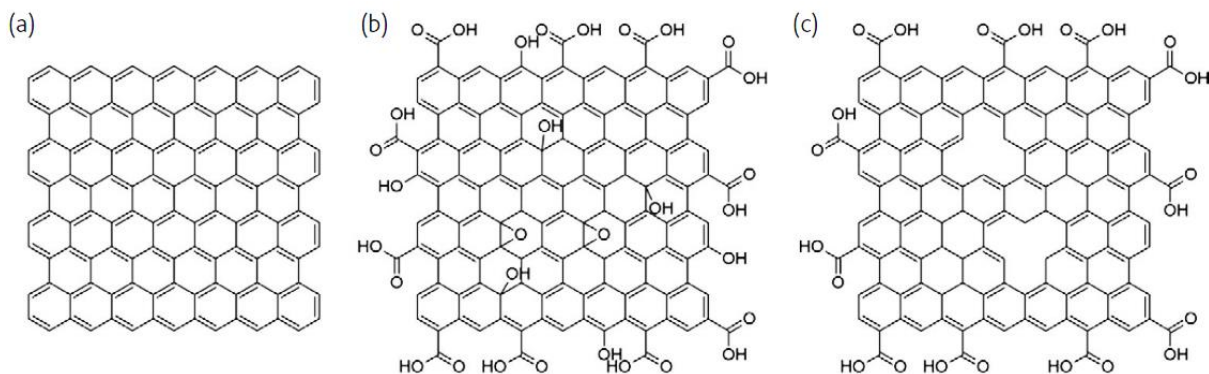


Figure 9. Two-dimensional molecular structure of a sheet of graphene (a) and proposed two-dimensional structures of GO (b) and RGO (c). Image used with permission from Reference 37.

In order to produce large area graphene samples, a chemical vapor deposition method was developed that could grow graphene samples much larger than mechanical exfoliation.³⁸ Unfortunately, both of these methods can be difficult and expensive, which has resulted in increased interest in graphene based materials such as GO and RGO (Figure9). GO is typically prepared by chemical exfoliation of graphite, which is significantly easier and more cost effective than the production of graphene.^{39,40} GO is structurally similar to graphene, except much of its conductivity has been disrupted by oxygen containing functional groups, such as alcohols, carboxylic acids, and epoxides.³⁴ The hydrophilic oxygen groups work to enhance GO solubility in aqueous solutions, which is ideal for interfacing it with PSI. The disrupted conjugation of GO can be partially restored, however, by reducing it to RGO. This process reestablishes much of graphene's conjugated π -orbital system, and can be accomplished using various reducing agents such as hydrazine monohydrate³⁹ or L-ascorbic acid.⁴¹

3.2 Interfacing Photosystem I with Graphene Oxide and Reduced Graphene Oxide

As previously reported, our group has found great success in generating photocurrent using thick, multilayer films of PSI.²¹ It was suspected, however, that despite this significant enhancement, many of the charge separations that were being created in the films were not adding to the current because the electrons deep in the film could not be reached effectively by the electrochemical mediator. Therefore, we hypothesized that integrating the protein complexes into a conductive matrix could help facilitate additional electron transfer and increase the generated photocurrents of these multilayer films even further.

Little work has been done in the area of interfacing PSI proteins with carbon-based systems. In 2007, Carmeli *et al.* modified carbon nanotubes with PSI reaction centers,⁴² while in 2013 researchers in the Cliffel and Jennings groups successfully demonstrated photocurrent from PSI-modified graphene as a highly transparent electrode material.⁴³ Based on these successes, it was thought that RGO may be an effective matrix material to embed the protein in. Additionally, GO and RGO are affordable and easy to work with. The following work details these studies.

3.3 Results and Discussion

Photocurrent production was measured for these electrodes by performing photochronoamperometry (Figure 10) and cyclic voltammetry (CV) (Figure 11) experiments. From the photochronoamperometry data we saw a clear enhancement in photocurrent from the

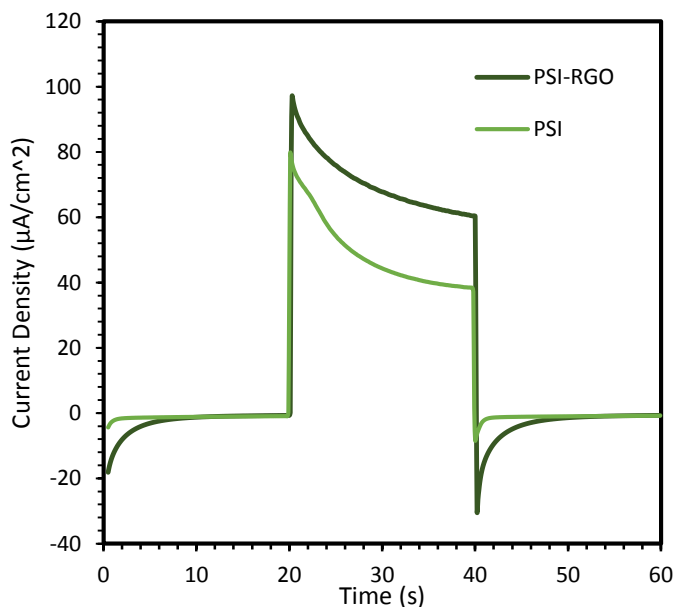


Figure 10. Photochronoamperometry curves of PSI and PSI-RGO composite films on etched p-Si substrates, using 2 mM MV as a mediator and 100 mM KCl as a supporting electrolyte, illuminated from 20-40 s.

PSI-RGO composite film compared to a film of only PSI of $\sim 30 \mu\text{A}/\text{cm}^2$. This enhancement was attributed to increased conductivity in the film due to the RGO matrix.

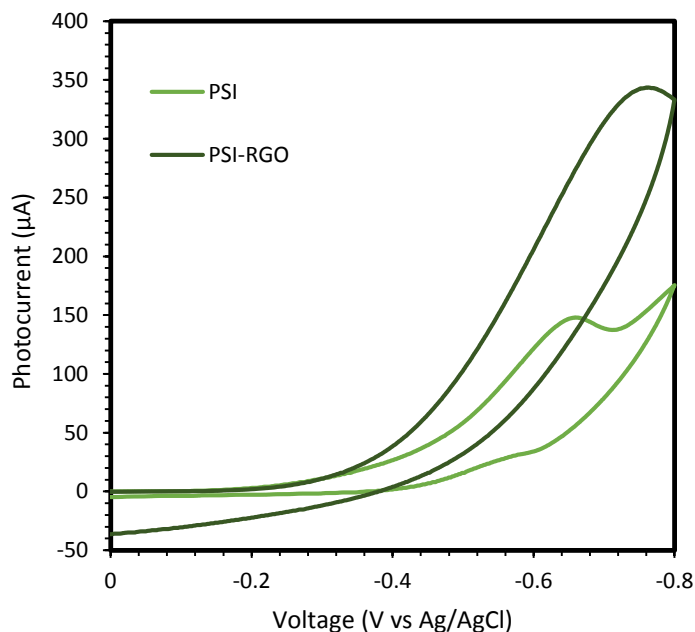


Figure 11. Cyclic voltammogram of PSI and PSI-RGO composite films on etched p-Si, using 2 mM MV as a mediator and 100 mM KCl as a supporting electrolyte, under constant illumination.

The cyclic voltammogram of PSI-RGO strengthens our hypothesis by showing increased photocurrent production from the composite electrodes vs PSI films only.

Additional work in our research group was later performed to expand on these findings. A larger systematic study of PSI embedded into RGO and even GO composite films was performed which showed that PSI-GO composites produced higher photocurrents than even PSI-RGO ($\sim 140 \mu\text{A}/\text{cm}^2$) in photochronoamperometric studies.⁴⁴ Linear sweep voltammetry was also performed which confirmed the higher photocurrent density and revealed that the PSI-GO films positively shifted the reduction potential of the mediator. Therefore, the increased photocurrent of PSI-GO was attributed to the shifted reduction potential as well as the film's

ability to increase the local concentration of mediator at the electrode by way of its charged functional groups, a feature that RGO lacks.⁴⁴

3.4 Conclusions

We have shown that functional, biohybrid electrodes can be produced by embedding PSI protein complexes into conductive RGO and GO matrixes. These films exhibit enhanced photocurrent compared to PSI which is attributed to enhanced conductivity for the facilitation of electron transfer to the mediator (RGO) and a shift in the reduction potential of the mediator and increased local mediator concentration (GO). These conductive, carbon-based matrix materials could potentially be used with other redox active proteins for the production of different biohybrid electrodes or biosensors.

3.5 Experimental

3.5.1 Photosystem I Extraction and Isolation

Photosystem I protein complexes were extracted and isolated according to the procedure discussed in Chapter 2. Briefly, PSI proteins were extracted from baby spinach by maceration and centrifugation in buffer and purified using a chilled hydroxylapatite column. The protein was then dialyzed at a 1:2000 extract to water ratio to remove excess surfactant.

3.5.2 Preparation of PSI-RGO Composites

Aqueous 5 mg/mL GO (graphene-supermarket.com) was diluted to 0.5 mg/mL and reduced to RGO using 5 mg/mL L-ascorbic acid (AA) at room temperature overnight, as

demonstrated by Zhang *et al.*⁴¹ The reduction progress was monitored using UV-Vis spectroscopy (Figure 12). The characteristic red-shift of GO peak absorption at 230 nm to the RGO peak absorption at 265 nm was used to confirm the reduction had been carried out successfully.

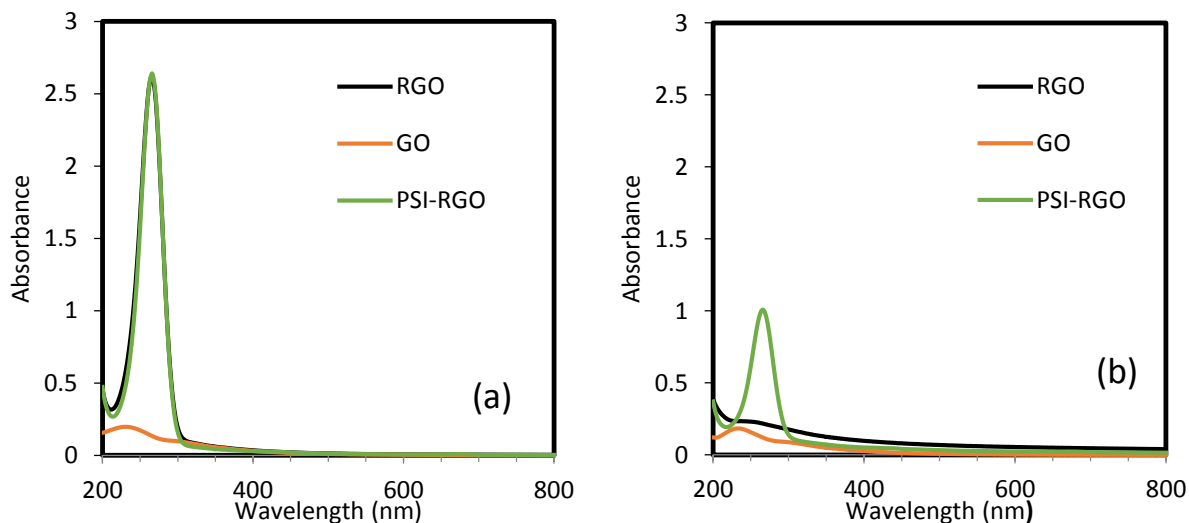


Figure 12. UV-Vis spectra of the reduction of GO to RGO at 0 h (a) and 24 h (b). GO represents an initial solution of only 0.5 mg/mL GO, RGO represents an initial solution of 0.5 mg/mL GO with 5 mg/mL AA, and PSI-RGO represents an initial solution 0.5 mg/mL GO with 5 mg/mL AA and PSI protein extract. The shift in peak absorption (b) from 230 nm to 265 nm is characteristic of the reduction from GO to RGO.

3.5.3 Hydrofluoric Acid Etching of Silicon Substrates

Boron doped silicon wafers (University Wafer) were cut into the desired size. A 2% hydrogen fluoride solution was used to etch the surface oxide layer that naturally develops on the silicon substrates when exposed to air. The substrates were then washed with DI water and dried under N₂.

3.5.4 Deposition of Composite Films onto Etched Silicon Substrates

All films were deposited onto the etched p-Si substrates according to the multilayer, dropcast deposition method described in Chapter 2. Briefly, 50 μL of composite solution were deposited onto the substrate and held under vacuum for 15 min until dry. This was repeated 3 times to achieve the desired film thickness.

3.5.5 Raman Analysis of Composite Films

Raman scattering spectra were collected using a Thermo Scientific DXR Raman confocal microscope. GO and RGO show two Raman peaks at 1300 cm^{-1} and 1580 cm^{-1} . A characteristic decrease in the ratio of these peaks can be observed to further verify the reduction. Images of the films were taken using the microscope (Figure 13).

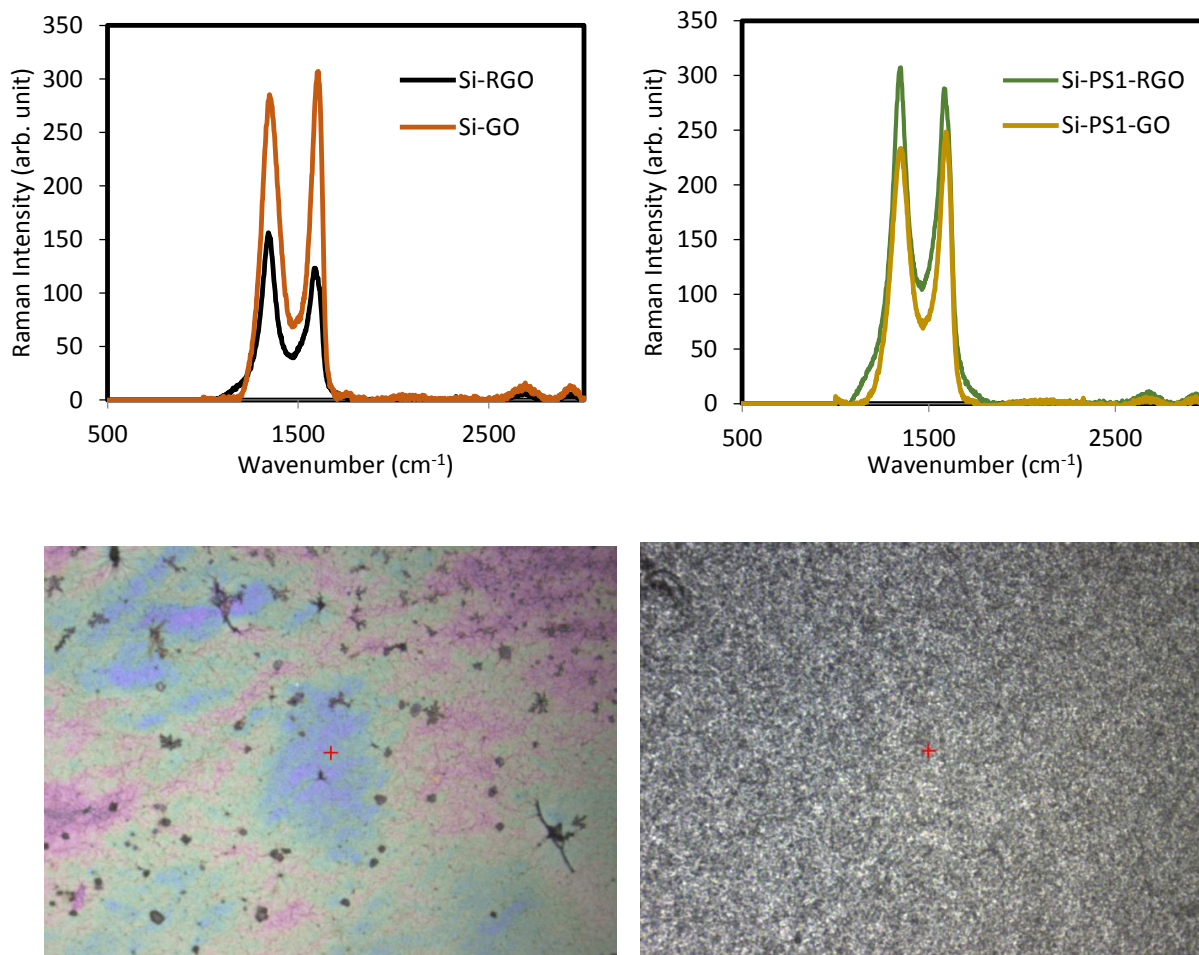


Figure 13. Top: Raman spectra showing the characteristic decrease in the ratio of peak intensities (1300 cm^{-1} and 1580 cm^{-1}) after reduction of GO to RGO. Bottom: Confocal microscope images of PSI-GO (left) and PSI-RGO (right) composite films on p-Si substrates.

3.5.6 Profilometry

Film thicknesses were measured using a Veeco Dektak 150 stylus profilometer. A line was scratched across the film down to the substrate to serve as a baseline. The stylus was moved across the film and baseline to obtain an accurate film thickness.

3.5.7 Electrochemical Analysis of Composite Biohybrid Electrodes

A 3-electrode setup and illumination source identical to that described in Chapter 2 were utilized to perform the electrochemical analyses of these PSI-RGO composite films using 2 mM methyl viologen as a mediator species. Photochronoamperometry experiments were performed at the experimentally determined dark OCP with a sample interval of 0.1 s. Cyclic voltammetry experiments were performed using a scan window of 0.8 V to -0.8 V with a scan rate of 0.1 V/s.

CHAPTER 4

Reduced Graphene Oxide as a Transparent Electrode

with Photosystem I Films

4.1 Transparent Electrodes and Opaque Mediators

Previous work in our group has shown that the selection of electrochemical mediator species is critical for maximizing photocurrent in PSI-based biohybrid electrodes.³² This study showed that mediators with increasingly positive formal potentials produced higher photocurrents, with a few exceptions: MB and DCPIP. This break in the trend was attributed to the fact that both species form dark blue solutions that absorb visible light in much of the same region as PSI. Because the PSI-modified electrode had to be illuminated through the mediator, much of the illumination source was lost before it reached the photoactive film, resulting drastically lowered photocurrent densities. Therefore, a conductive, transparent electrode material is desirable so that the deposited photoactive protein films could be illuminated from the back (through the electrode), allowing the use of highly colored mediators such as MB and DCPIP.

4.2 Reduced Graphene Oxide as a Transparent, Conductive Electrode

Graphene is an interesting material due to its high thermal and electrical conductivity, high elasticity, and high transparency in the visible region.³³⁻³⁵ A previous collaboration between the Cliffel, Jennings, and Bolotin groups demonstrated that monolayer graphene could be used as

a transparent electrode for photoactive PSI monolayers.⁴³ Unfortunately, these graphene substrates were expensive and time consuming to produce. Additionally, the study only used PSI monolayers. Based on these results, we hypothesized that thin films of RGO would maintain much of the conductivity and transparency of monolayer graphene while being easy and inexpensive to produce and able to support multilayer films of PSI.

4.3 Results and Discussion

Electrodes were prepared by spincoating GO onto functionalized glass slides and reducing it to RGO using hydrazine vapor. Multilayer films of PSI were deposited onto the electrodes and electrochemical measurements were taken. Photocurrent was measured using photochronoamperometry, with the photoactive protein films being illuminated through the RGO electrode, rather than through the mediator (Figure 14).

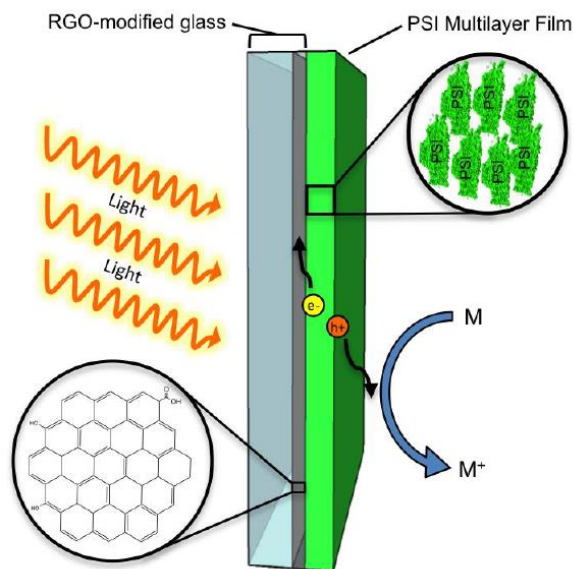


Figure 14. Diagram of the PSI-modified RGO electrode that shows the flow of electrons from the mediator (M) through the protein film to the working electrode. Image taken from Reference 45, pending publication in Langmuir.

For all mediators tested, we observed negative photocurrents, indicating electrons are flowing from the mediator into the electrode, or oxidizing the mediator species.

Photochronoamperometry of an unmodified RGO electrode was done to determine the photoactivity of the electrode itself. While the RGO electrode produces significant photocurrent density ($\sim -0.71 \mu\text{A}/\text{cm}^2$), we still see a nearly three-fold enhancement when modified with the PSI multilayers ($\sim 1.8 \mu\text{A}/\text{cm}^2$) (Figure 15). The photoactivity of several mediator species was also measured. Specifically, current densities produced by 2 mM DCPIP were negligible ($\sim -0.2 \mu\text{A}/\text{cm}^2$) (Figure 16). The remarkably high photocurrents produced by 1 mM ferricyanide/1 mM ferrocyanide were unexpected compared to the other darker, more opaque mediators. These experiments show that the current densities we see produced by the RGO-PSI electrodes are almost entirely produced by the photoactive protein film and are comparable to those seen from PSI-modified gold electrodes in our group,²¹ and indicate that the RGO electrodes behave like a traditional metallic electrode. In addition, the photocurrent is maintained for extended periods of

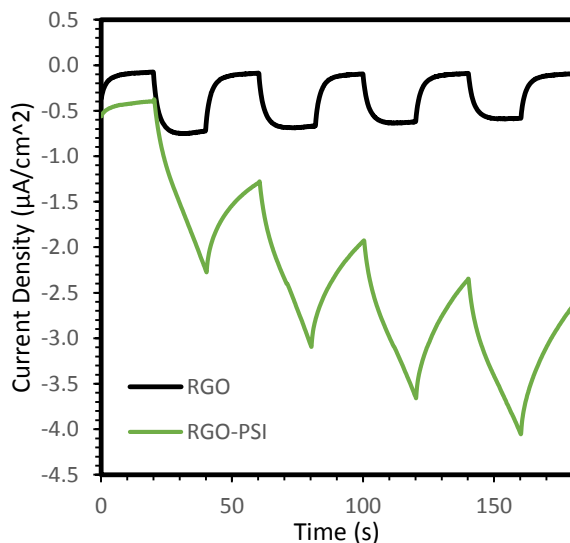


Figure 15. Photochronoamperometric measurements of RGO and PSI-modified RGO electrodes with 2 mM DCPIP as a mediator and 100 mM KCl as supporting electrolyte, Ag/AgCl as a reference electrode, and Pt mesh as a counter electrode. All samples were illuminated for 20 s intervals beginning at 20 s.

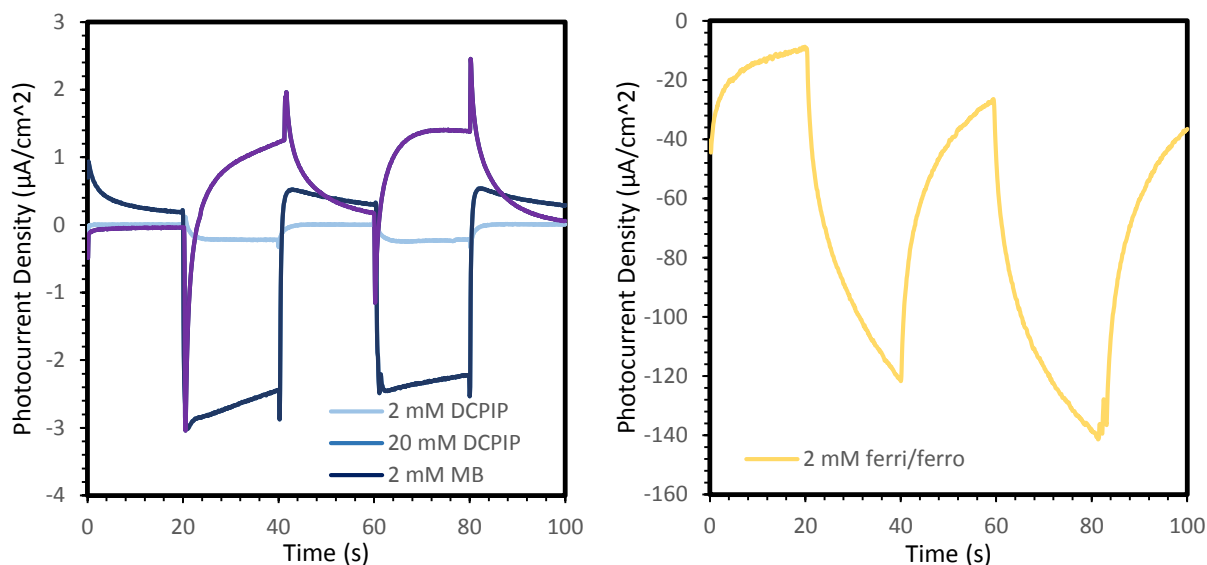


Figure 16. Photochronoamperometric measurements of (left) 2 mM DCPIP, 20 mM DCPIP, and 2 mM MB mediators and (right) 1 mM ferricyanide/1 mM ferrocyanide using a transparent FTO electrode and 100 mM KCl as a supporting electrolyte. All samples were illuminated for 20 s intervals beginning at 20 s.

time. The shape of the PSI-modified electrodes and the drift in the photocurrent to more negative values is undesirable, but similar experiments performed by others in our group showed photochronoamperometric curves without these faults, indicating that the electrodes do, indeed, function as expected. The thickness of the RGO electrode was determined using a stylus profilometer and showed that each deposition of RGO added ~50 nm to the thickness (Figure 17). The transparency of the electrode was measured using a powermeter in order to determine how much light was lost to photoexcitation of the electrode before reaching the PSI multilayer (Figure 18). Unimpeded light intensity was measured as 0.78 ± 0.08 W. Passing light through the RGO electrode reduced its intensity by an order of magnitude. This method is far superior to passing light through the mediator, as has been traditionally done, which allows only ~3% of the incident light to reach the photoactive protein film.

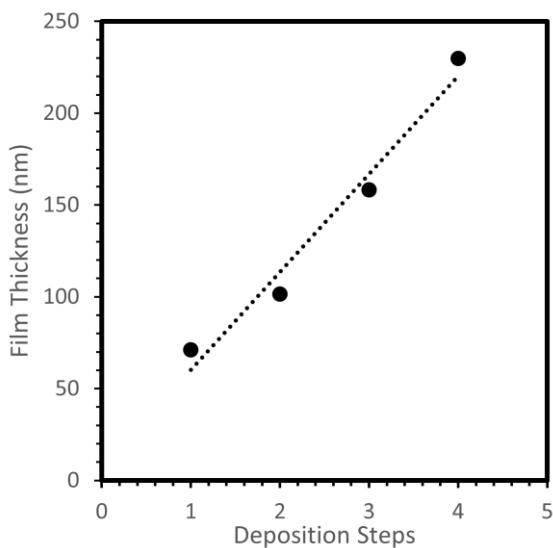


Figure 17. Film thickness of RGO electrodes as a function of the number of deposition steps applied. Each deposition produces a ~50 nm growth.

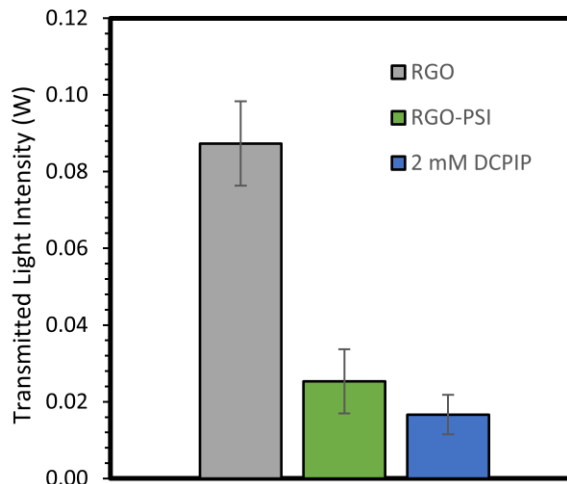


Figure 18. The average power measurements ($n=3$) of the transmitted light intensity through the RGO electrode, PSI-modified RGO electrode, and 2 mM DCPIP.

4.4 Conclusions

We have successfully demonstrated that RGO can be utilized as a transparent, conductive electrode for interfacing with thick, photoactive multilayer films of PSI. These electrodes allow for illumination of the protein through the electrode rather than the mediator, offering the option of using highly colored mediator solutions which were previously unusable due to their absorption spectra overlapping with that of PSI in the visible region. Photocurrents from these PSI-modified RGO electrodes were comparable to those seen from PSI-modified metal electrodes. The metallic nature of the RGO electrodes could potentially be limiting photocurrents, however, due to the mixed orientation of the proteins in the film effectively negating much of the current. Future work with this material could push photocurrent values even higher by controlling protein orientation. Additionally, increasing mediator concentration, possible due to illumination through the electrode, should see significant photocurrent increases.

4.5 Experimental

4.5.1 Photosystem I Extraction and Isolation

Photosystem I protein complexes were extracted and isolated according to the procedure discussed in Chapter 2. Briefly, PSI proteins were extracted from baby spinach by maceration and centrifugation in buffer and purified using a chilled hydroxylapatite column. The protein was then dialyzed at a 1:2000 extract to water ratio to remove excess surfactant.

4.5.2 Production of RGO Electrodes

Transparent RGO electrodes were prepared following a slightly modified version of a method previously reported by Becerril *et al.*⁴⁶ Glass slides were cut to the desired size and washed with water, then acetone, then ethanol (EtOH) and dried with N₂. The slides were then submerged in a 1% v/v aminopropyl triethoxysilane solution for 1 h in a Parafilm® sealed container. The slides were then removed from the solution and rinsed with EtOH and dried with N₂. A 5 mg/mL GO in EtOH solution was prepared and 500 µL spuncoat onto the functionalized glass slide at 800 rpm for 4 min. The GO films were then reduced for 1 h at 70 °C in a Parafilm® sealed container in the presence of 1 mL of hydrazine monohydrate. The reduction could be confirmed visually by a darkening in the color of the slides (Figure 19).

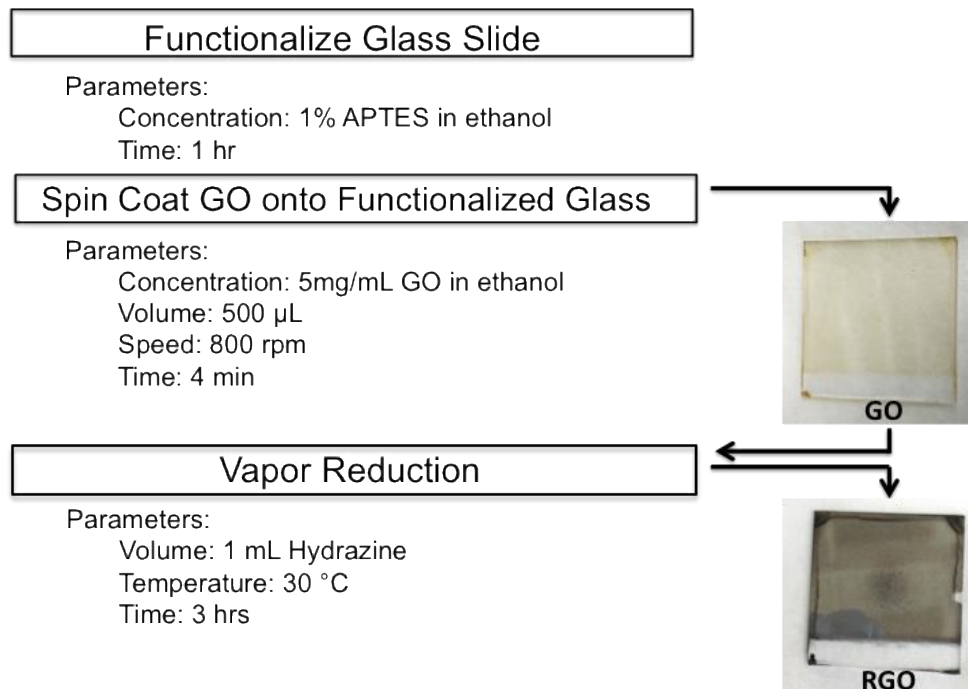


Figure 19. Summary of the method used for the production of conductive RGO electrodes on glass substrates. Image taken from Reference 45, pending publication in Langmuir.

4.5.3 Deposition of PSI Multilayer Films on RGO Electrodes

All films were deposited onto the RGO electrodes according to the multilayer, dropcast deposition method described in Chapter 2. Briefly, 50 μ L of PSI protein extract were deposited onto a 0.283 cm^2 exposed area of the substrate and held under vacuum for 15 min until dry. This was repeated 3 times to achieve the desired film thickness.

4.5.4 Electrochemical Analyses of PSI-modified RGO Electrodes

A 3-electrode setup and illumination source identical to that described in Chapter 2 were utilized to perform the electrochemical analyses of these PSI-modified RGO electrodes, with the exception of illumination occurring through the electrode rather than through the mediator. A 2 mM DCPIP solution was used as an electrochemical mediator. Photochronoamperometry

experiments were performed at the experimentally determined dark OCP with a sample interval of 0.1 s and an illumination period of 20 s.

4.5.5 Profilometry

Film thicknesses were measured using a Veeco Dektak 150 stylus profilometer. A line was scratched across the film down to the substrate to serve as a baseline. The stylus was moved across the film and baseline to obtain an accurate film thickness.

4.5.6 Transmitted Light Intensity Measurements

A Coherent Radiation 210 power meter was used to measure the intensity of light transmitted through different, consecutive layers of the electrochemical cell. The meter was positioned at a distance equal to that of the photoactive film from the light source. A foil with a hole $\sim 0.283 \text{ cm}^2$ was used to limit the light reaching the meter to an amount more closely representative of that which would be incident on the photoactive protein film. The light was turned on and the measurement was recorded. This was done for all consecutive combinations of

	Transmitted Light (W)
Unimpeded light	0.78 ± 0.08
Cell cover	0.69 ± 0.02
RGO	0.087 ± 0.01
RGO-PSI	0.025 ± 0.01
2 mM DCPIP	0.017 ± 0.00

Table 1. Power of transmitted light passed through subsequent layers of the electrochemical cell (n=3), beginning with unimpeded light and continuing additively down the column to RGO-PSI. Data for 2 mM DCPIP was obtained by passing light through the “front” of the cell filled with the mediator solution, using glass as the “electrode.”

each layer of the electrochemical cell, i.e. the cell cover; the cell cover and RGO electrode; the cell cover, RGO electrode, and PSI multilayer film; etc (Table 1).

REFERENCES

- (1) Dong, Z.; Kennedy, S. J.; Wu, Y. *J. Power Sources* **2011**, *196* (11), 4886-4904.
- (2) Nocera, D. G.; Nash, M. P. *Proc. Natl. Acad. Sci. U. S. A.* **2007**, *104*, 15729–15735.
- (3) Lewis, N. S. *Science* **2007**, *315*, 798–801.
- (4) Hagfeldt, A.; Boschloo, G.; Sun, L.; Kloo, L.; Pettersson, H. *Chem. Rev.* **2010**, *110*, 6595–6663.
- (5) Hall, D. O. *Photosynthesis*; Sixth Edit.; Cambridge University Press: Cambridge, **1999**; pp. 1–2.
- (6) Nelson, N.; Yocum, C. F. *Annu. Rev. Plant Biol.* **2006**, *57*, 521–565.
- (7) Golbeck, J. H. *Annu. Rev. Plant Physiol. Plant Mol. Biol.* **1992**, *43*, 293–324.
- (8) Hogewoning, S. W.; Wientjes, E.; Douwstra, P.; Trouwborst, G.; Van, I. W.; Croce, R.; Harbinson, J. *Plant Cell* **2012**, *24*, 1921–1935.
- (9) Nelson, N.; Ben-Shem, A. *Nat. Rev. Mol. Cell Biol.* **2004**, *5*, 971–982.
- (10) Greenbaum, E. *Science* **1985**, *230*, 1373–1375.
- (11) Millsaps, J. F.; Bruce, B. D.; Lee, J. W.; Greenbaum, E. *Photochem. Photobiol.* **2001**, *73*, 630–635.
- (12) Lee, J. W.; Greenbaum, E. Bioelectronics and biometallo catalysis for production of fuels and chemicals by photosynthetic water splitting. *Applied Biochemistry and Biotechnology*, **1995**, *51-52*, 295–305.
- (13) Iwuchukwu, I. J.; Vaughn, M.; Myers, N.; O’Neill, H.; Frymier, P.; Bruce, B. D. *Nat. Nanotechnol.* **2010**, *5*, 73–79.
- (14) Lee, I.; Lee, J. W.; Greenbaum, E. *Phys. Rev. Lett.* **1997**, *79*, 3294–3297.
- (15) Munge, B.; Das, S. K.; Ilagan, R.; Pendon, Z.; Yang, J.; Frank, H. A.; Rusling, J. F. *J. Am. Chem. Soc.* **2003**, *125*, 12457–12463.
- (16) Das, R.; Kiley, P. J.; Segal, M.; Norville, J.; Yu, A. A.; Wang, L. Y.; Trammell, S. A.; Reddick, L. E.; Kumar, R.; Stellacci, F.; Lebedev, N.; Schnur, J.; Bruce, B. D.; Zhang, S. G.; Baldo, M. *Nano Lett.* **2004**, *4*, 1079–1083.
- (17) Ciobanu, M.; Kincaid, H. A.; Jennings, G. K.; Cliffel, D. E. *Langmuir* **2004**, *21*, 692–698.

- (18) Ciobanu, M.; Kincaid, H. A.; Lo, V.; Dukes, A. D.; Jennings, G. K.; Cliffel, D. E. *J. Electroanal. Chem.* **2007**, *599*, 72–78.
- (19) Faulkner, C. J.; Lees, S.; Ciesielski, P. N.; Cliffel, D. E.; Jennings, G. K. *Langmuir* **2008**, *24*, 8409–8412.
- (20) Ciesielski, P. N.; Scott, A. M.; Faulkner, C. J.; Berron, B. J.; Cliffel, D. E.; Jennings, G. K. *ACS Nano* **2008**, *2*, 2465–2472.
- (21) Ciesielski, P. N.; Faulkner, C. J.; Irwin, M. T.; Gregory, J. M.; Tolk, N. H.; Cliffel, D. E.; Jennings, G. K. *Adv. Funct. Mater.* **2010**, *20*, 4048–4054.
- (22) Ciesielski, P. N.; Hijazi, F. M.; Scott, A. M.; Faulkner, C. J.; Beard, L.; Emmett, K.; Rosenthal, S. J.; Cliffel, D.; Jennings, G. K. *Bioresour. Technol.* **2010**, *101*, 3047–3053.
- (23) Leblanc, G.; Chen, G.; Gizzie, E. A.; Jennings, G. K.; Cliffel, D. E. *Adv. Mater.* **2012**, 1–4.
- (24) Leblanc, G.; Gizzie, E.; Yang, S.; Cliffel, D. E.; Jennings, G. K. *Langmuir* **2014**.
- (25) Reeves, B. S. G.; Hall, D. O. *Methods Enzymol.* **1980**, *69*, 85–94.
- (26) Shiozawa, J. A.; Alberte, R. S.; Thornber, J. P. *Arch. Biochem. Biophys.* **1974**, *165*, 388–397.
- (27) Kincaid, H. A.; Niedringhaus, T.; Ciobanu, M.; Cliffel, D. E.; Jennings, G. K. *Langmuir* **2006**, *22*, 8114–8120.
- (28) Leblanc, G. Biohybrid Electrodes Based on Photosystem I for Solar Energy Conversion, Vanderbilt University, **2014**, pp. 1–115.
- (29) Gunther, D.; LeBlanc, G.; Cliffel, D. E.; Jennings, G. K. *Ind. Biotechnol.* **2013**, *9*, 37–41.
- (30) Baba, K.; Itoh, S.; Hastings, G.; Hoshina, S. . *Photosynth. Res.* **1996**, *47*, 121–130.
- (31) Porra, R. J. *Photosynth. Res.* **2002**, *73*, 149–156.
- (32) Chen, G.; LeBlanc, G.; Jennings, G. K.; Cliffel, D. E. *J. Electrochem. Soc.* **2013**, *160*, H315–H320.
- (33) Geim, A. K. *Science* **2009**, *324*, 1530–1534.
- (34) Wang, H.-X.; Wang, Q.; Zhou, K.-G.; Zhang, H.-L. *Small* **2013**, *9*, 1266–1283.
- (35) Nair, R. R.; Blake, P.; Grigorenko, A. N.; Novoselov, K. S.; Booth, T. J.; Stauber, T.; Peres, N. M. R.; Geim, A. K. *Science*. **2008**, *320*, 1308.

- (36) Novoselov, K. S.; Geim, A. K.; Morozov, S. V.; Jiang, D.; Zhang, Y.; Dubonos, S. V.; Grigorieva, I. V.; Firsov, A. A. *Science*. **2004**, *306*, 666–669.
- (37) Kim, J.; Kim, F.; Huang, J. *Mater. Today* **2010**, *13*, 28–38.
- (38) Reina, A.; Jia, X.; Ho, J.; Nezich, D.; Son, H.; Bulovic, V.; Dresselhaus, M. S.; Jing, K. *Nano Lett.* **2009**, *9*, 30–35.
- (39) Dreyer, D. R.; Park, S.; Bielawski, C. W.; Ruoff, R. S. *Chem. Soc. Rev.* **2010**, *39*, 228–240.
- (40) Dikin, D. A.; Stankovich, S.; Zimney, E. J.; Piner, R. D.; Dommett, G. H. B.; Evmenenko, G.; Nguyen, S. T.; Ruoff, R. S. *Nature* **2007**, *448*, 457–460.
- (41) Zhang, J.; Yang, H.; Shen, G.; Cheng, P.; Zhang, J.; Guo, S. *Chem. Commun.* **2010**, *46*, 1112–1114.
- (42) Carmeli, I.; Mangold, M.; Frolov, L.; Zebli, B.; Carmeli, C.; Richter, S.; Holleitner, A. W. *Adv. Mater.* **2007**, *19*, 3901–3905.
- (43) Gunther, D.; LeBlanc, G.; Prasai, D.; Zhang, J. R.; Cliffel, D. E.; Bolotin, K. I.; Jennings, G. K. *Langmuir* **2013**, *29*, 4177–4180.
- (44) LeBlanc, G.; Winter, K. M.; Crosby, W. B.; Jennings, G. K.; Cliffel, D. E. *Adv. Energy Mater.* **2014**, in press.
- (45) Darby, E.; Leblanc, G.; Gizzie, E. A.; Winter, K. M.; Jennings, G. K. *Langmuir* Under Review.
- (46) Becerril, H. A.; Mao, J.; Liu, Z.; Stoltenberg, R. M.; Bao, Z.; Chen, Y. *ACS Nano* **2008**, *2*, 463–470.

Kevin Winter

Curriculum Vitae

Vanderbilt University | 107 Acklen Park Drive, Apt. 205 | Nashville, TN 37203

E-mail: kevin.m.winter@vanderbilt.edu; kvnwntr@gmail.com

Education

M.S. Chemistry, Vanderbilt University, August 2014 GPA: 3.66

Thesis Title: *Integration of Photosystem I with Carbon-Based Materials for Solar Energy Conversion Devices*

B.S. Chemistry, Kentucky Wesleyan College, May 2012 GPA: 4.00

Research Experience

Graduate Research Spring 2013- Present

Vanderbilt University, Nashville, TN

Developed carbon-based biohybrid electrodes and incorporated Photosystem I with them for solar energy conversion. Devices and materials were analyzed using electrochemical methods, UV-Vis spectroscopy, Raman spectroscopy, and profilometry.

Advisor: David Cliffler, Ph.D.

Research Internship Fall 2011

Owensboro Cancer Research Program, Owensboro, KY

Studied the effect of calcium signaling on the maintenance of hematopoietic stem cells.

Techniques utilized include extensive cell culturing, Western blots, and PCR and RT-PCR assays.

Advisor: Uma Sankar, Ph.D.

Awards and Honors

Vanderbilt Institute of Chemical Biology Fellowship 2012-2013

Chemistry Alumni Award 2011

American Chemical Society Chemistry Award 2010

Chemical Rubber Company Chemistry Award 2009

Teaching Experience

Teaching Assistant- Vanderbilt University Fall 2013-Spring 2014

Managed classes of 20-25 first year undergraduate students in a chemistry lab setting; developed and presented lectures over the coursework for the week; assisted students through challenges that arose during their experiments; held office hours to meet with students outside of class for homework tutoring and test preparation; and administered and graded lab work and exams.

Vanderbilt Student Volunteers for Science Team Leader Fall 2013-Spring 2014

Led a team of 4 Vanderbilt University students to deliver hands-on science lessons and demonstrations to middle school students; led discussions with students over the lesson and helped them apply it to their everyday lives.

Lab Proctor/Tutor- Kentucky Wesleyan College

Fall 2009-Spring 2012

Managed General and Organic Chemistry labs while students were working; demonstrated lab procedures and assisted students; and graded lab reports. Tutored Kentucky Wesleyan and local high school students in upper and lower level chemistry and math, as well as writing.

Publications

- (1) LeBlanc, G., Winter, K. M., Crosby, W. B., Jennings, G. K., Cliffel, D. E. Integration of Photosystem I with Graphene Oxide for Photocurrent Enhancement. *Adv. Energy Mater. In Press*.

Publications in Preparation

- (2) Darby, E., LeBlanc, G., Gizzie, E. A., Winter K. M., Jennings, G. K., Cliffel, D. E. Photoactive Films of Photosystem I on Transparent Reduced Graphene Oxide Electrodes. *Langmuir* Submitted.